

High-Energy Spectra From Black-Hole Candidates

T. Belloni^a

^aINAF-Osservatorio Astronomico di Brera, Via E. Bianchi 46, I-23807 Merate, Italy

Our knowledge of the high-energy emission spectra from black-hole candidates has increased enormously with missions like BeppoSAX and RossiXTE, thanks to their broad-band window. I present the main and most solid points of this current knowledge, both in terms of detailed spectral modeling of X-ray broad-band spectra, and more generally in relation to the “black-hole state paradigm”, which links spectral and timing properties of accretion disks. Finally, through the discussion of recent results on two systems, XTE J1650-500 and GX 339-4, I present evidence for a new view of the state paradigm.

1. Introduction

The launch of RossiXTE and BeppoSAX have opened a new era for our understanding of high-energy spectra from Black-Hole Candidates (BHC). On the one hand, the large number of pointings allowed by the flexibility of RXTE, both for transient and persistent systems, has allowed a thorough coverage of spectral (and timing) properties of these systems, in particular with respect to their state transitions. On the other hand, the broad-band capabilities of both satellites have given us high signal-to-noise ratio spectra over almost three decades in energy. This made it possible to study in detail the overall spectral distribution without leaving out any important component. In the following, after a brief description of the current status of the state-classification, I will first discuss some general issues about broad-band spectra of BHC, based on a few examples. Then, I will present detailed results on two systems observed with RXTE, XTE J1650-500 and GX 339-4, concluding with a new view of BH canonical states.

2. “Canonical states”

After a long history of changes, additions and removals, the author’s current picture of BH states is the following (see [36,37,30,10]).

- *LS*: Low/hard state. The energy spectrum is dominated by a power-law-like

component, with a photon index ~ 1.6 , which shows a clear high-energy cutoff at around ~ 100 keV. An additional weak very soft component, probably associated to the thermal disk, might be observable below 1 keV if the interstellar absorption is not too high.

- *HS*: High/soft state. The energy spectrum is dominated by a thermal component, usually modeled with a disk-blackbody component with a temperature of 1-2 keV. A weak power-law component is present, with a steeper photon index. No apparent high-energy cutoff is observed in high signal-to-noise spectra.
- *VHS/IS*: Very High/Intermediate state. The energy spectrum features both a thermal component similar to that observed in the HS and a hard power-law like component with photon index ~ 2.5 . The relative contribution of these two components to the 1-10 keV flux can vary between 10 and 90%.

In the above I did not discuss the presence of additional components as Compton reflection or iron lines/edges as I wanted to limit myself to the main components at play. Notice that I also did not mention variability features, which are important in the definition of states. This is intended, in order to focus the attention on to the spectral properties, although indeed in some case the

knowledge of timing properties would be necessary to assess the current state of a source.

After the results obtained on XTE J1550-564 [10], it is now clear that changes in the mass accretion rate are not sufficient to explain all state transitions, and that there must be a second parameter at play. The nature of this second parameter is at present unknown.

3. Broad-band X-ray spectra

The availability of better instruments and missions has put in our hands extraordinary tools to characterize broad-band spectra of BHC. In particular, the quality of BeppoSAX spectra obtained combining all four narrow-field instruments on board (LECS, MECS, HPGSPC and PDS) was extraordinary. The increase in quality however led to an increase in complication of the models used for spectral fitting. This makes it necessary to be much more careful in the modeling and interpretation, keeping also in mind that even the most detailed model cannot be but a simplification of reality. It is important to keep always in mind that X-ray spectral fitting at such energy resolutions yields an output that is strongly dependent on the assumptions made on the spectral model.

I show here three important examples.

3.1. XTE J1118+480

Probably the best source for a broad-band energy study was XTE J1118+480, as its low interstellar absorption allowed to detect flux down to well below 1 keV (see [2,4]). This source was observed only in the Low/Hard state. A large multi-wavelength campaign led to a detailed study of the Spectral Energy Distribution (SED), covering more than five orders of magnitude in energy [1,2,6,3].

The broad-band X-ray spectrum was studied from BeppoSAX observations [4,5]. The 0.1-200 keV spectrum was observed to be rather complex. The preferred best-fitting model consisted of a soft multi-temperature black body with inner temperature between 35 and 52 eV, observable only because of the low value for the interstellar absorption ($\sim 1.3 \times 10^{20} \text{ cm}^{-2}$), plus a thermal

Comptonization model with electron temperature $T_e \sim 85$ keV and optical depth around unity. In addition, a weak Compton reflection component was included (with covering fraction $R \sim 0.2$). The latter component indicated a low metallicity value ($Z/Z_\odot \sim 0.13$), consistent with the high galactic latitude of the system. This is a very complex model, involving an actual fit to the metallicity of the gas, which needs to be taken cautiously because of the number of theoretical assumptions needed to justify it. Indeed the first of the four spectra analyzed by [5] can be fitted also with a simpler model consisting of a multi-T black body and a power law with a high-energy cutoff. The magnitude of the deviations introduced by the Thermal Comptonization and Compton reflection models can be appreciated in Fig. 1, where the best fit to the complex model is shown in a deconvolved fashion. Nevertheless, the possibility of such a detailed fit from simultaneous data opens new possibilities for physical modeling of these spectra.

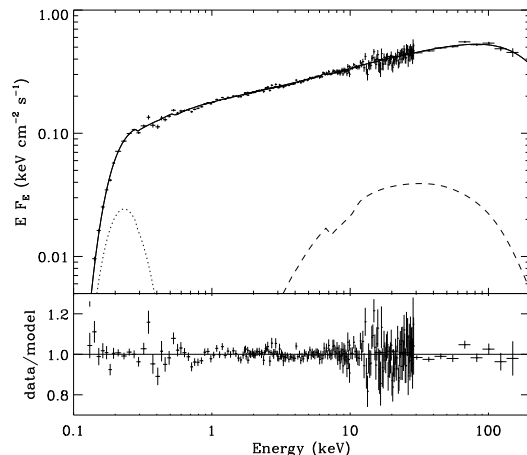


Figure 1. Deconvolved spectrum corresponding to the complex fit described in text for XTE J1118+480 (from [4]).

3.2. Cygnus X-1

It is difficult not to discuss the first and most famous BHC, Cygnus X-1. It was observed by

BeppoSAX both during its low/hard (LS) and high/soft (HS) states [7]. Again, the spectra are interpreted with a very complex model, rather similar in nature to the one discussed above. Detailed spectral modeling of a RXTE observation to Cyg X-1 in the hard state has been also reported, with simpler assumptions on the models (see [8]). What is interesting here is the comparison between the two states. The hard Comptonizing component is fitted to a purely thermal model in the case of the hard state, and with a hybrid model for the HS (see Fig. 2). Once again, the characterization of the hard component, thanks to the broad-band spectrum, goes into considerable detail.

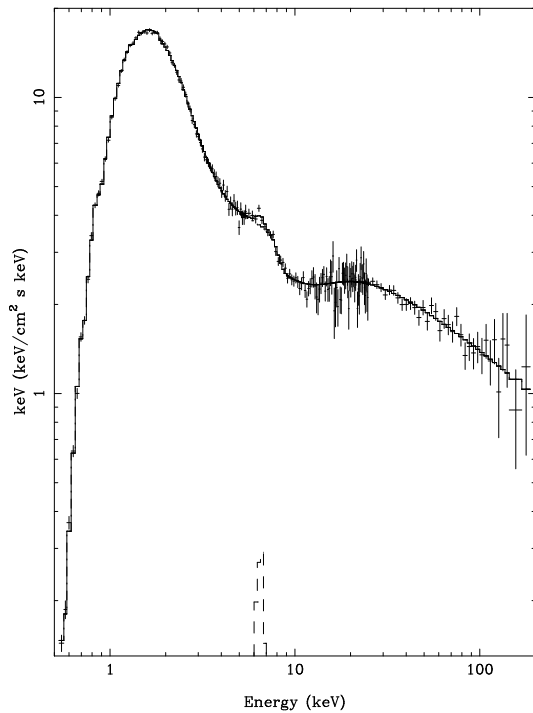


Figure 2. Deconvolved spectrum corresponding to the soft-state BeppoSAX observation of Cygnus X-1 (from [7]).

3.3. Thermal vs. non-thermal

The different nature of the hard component in different states had been discovered earlier (see e.g. [34]). An important survey of a number of BHC made with OSSE showed clearly that the presence of an ultrasoft component in the 1-10 keV range was associated to the lack of a detectable high-energy cutoff in the high-energy spectra up to 1 MeV, indicating a probable non-thermal origin [9]. A collection of spectra can be seen in Fig. 3.

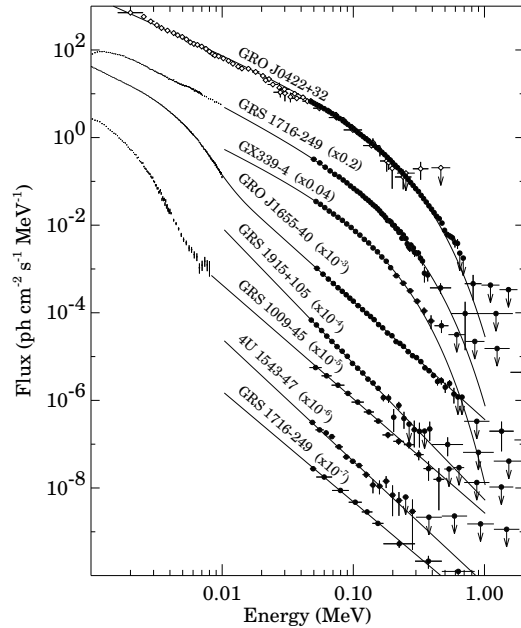


Figure 3. Deconvolved 1 keV-1 MeV spectra of a number of BHC observed by OSSE and other instruments (from [9]).

It is important to notice that it is not clear whether the spectra with no high-energy cutoff correspond to the soft/high state or to the very high/intermediate state (see [10]). It is therefore possible that also VHS/IS high-energy spectra have a non-thermal origin.

3.4. GRS 1915+105

This source shows the most complex phenomenology ever observed in X-ray binaries (see [11]). However, there is evidence that, at least most of the time, the source is in something similar to the VHS of more standard systems [12,13]. A combination of RXTE and OSSE data has shown that both in its B and C states, the hard component of GRS 1915+105 does not show any high-energy cutoff up to 0.9 MeV [14]. The OSSE spectra can be seen in Fig. 4.

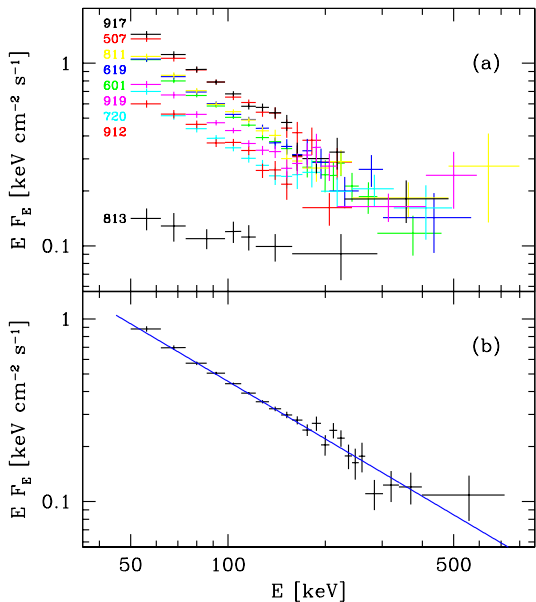


Figure 4. Top panel: nine OSSE spectra of GRS 1915+105 deconvolved with a power law. Bottom panel: average spectrum (from [14]).

3.5. Which component?

From the data shown above, it would seem that the component observed in the VHS is associated to that of the soft state and not to the thermal spectrum observed in the hard state. However, this is in contradiction with the properties of the timing variability, which shows properties gradually changing from the hard to the very high state

(see e.g. [15]). In other words, the timing results associate the VHS hard component to that seen in the HS, while spectra considerations connect it with that seen in the LS. This inconsistency needs to be resolved in order to present a clear view for the development of theoretical models. Integral is probably the mission that will give definite answers on the spectral side (see [16]).

4. BH transients: two recent examples

The best way to obtain information about states and state-transitions is to observe transient systems with dense campaigns that allow to monitor the timing/spectral properties of these systems for a whole outburst. In this way, one obtains a more coherent view of the properties of accretion in these systems, a more promising approach than the extremely detailed spectral fitting to a small number of observations are shown above. I outline here the basic results obtained on two systems, based on a large number of RXTE observations [23,24,15,26,25,35].

4.1. XTE J1650-500

This transient was discovered by the ASM/RXTE in September 2001, when an outburst lasting about fifteen months started. Follow-up observations showed a hard spectrum, strong variability, low and high frequency QPOs, and a relativistic skewed iron line suggesting the presence of a Kerr black hole [17,18,19,20,21]. The final portion of the outburst was studied by [22].

For the bright part of the outburst, more than one observation per day was performed with RXTE, yielding the most complete coverage of such a transient. The full spectral and timing analysis is presented in [23,24]. Here I show the basic evolution of the outburst. The PCA light curve and the corresponding X-ray hardness evolution (the hardness ratio is defined as the ratio of the counts in the 4.5-7.9 keV band to those in the 2.5-4.6 keV band) is shown in Fig. 5.

The density of the coverage is evident, as is the large range of spectral variations. A better view of these variations can be obtained by a Hardness-Intensity diagram (HID) (see Fig. 6). The source

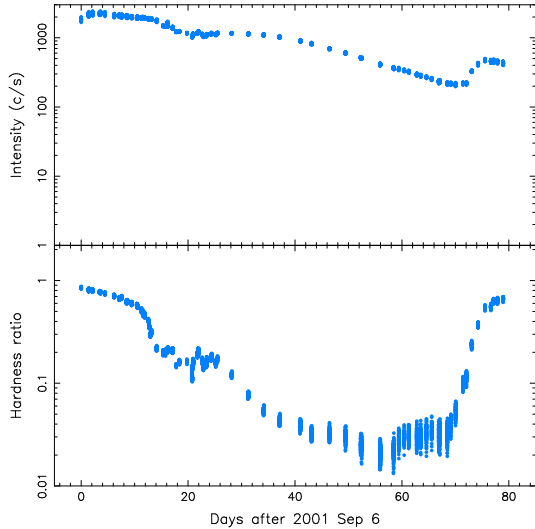


Figure 5. Top panel: PCA slight curve (PCU2 only) for the XTE J1650-500 RXTE campaign. Each point is accumulated over 16 s. Bottom panel: corresponding hardness curve (see text). (from [24]).

starts at the upper right corner, already at a bright level and hard, then moves left softening gradually. After a drop in count rate, it stabilizes for about ten days on to a small diagonally-shaped region of the HID. After this, it follows a vertical line as it becomes steadily fainter and slightly softer, to enter another horizontal hardening line. Not shown here, in the last part of the outburst, the flux decreases considerably, while the hardness remains approximately at the values found at the beginning of the outburst. Detailed spectral analysis in terms of the two main components shows that on the two horizontal tracks, both a soft and a hard component are present, with the hard one dominating the flux. During the stable interval, it is the soft component that dominates. Finally, along the vertical track, the hard component is very weak and almost all the flux comes from the soft component. This spectral evolution can be seen in Fig. 7. The four panels show for four representative PCA observa-

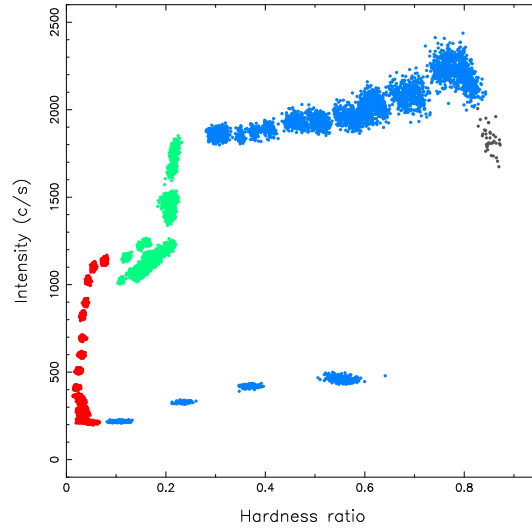


Figure 6. Hardness-Intensity diagram for XTE J1650-500 (PCU2 only) corresponding to the points shown in Fig. 5. (from [24]).

tions the ratio of the energy spectrum over that of the first observation, where the spectrum was dominated by a flat power law. Panel *A* corresponds to an observation from the top track in Fig. 6: here the ratio indicates a power-law spectrum similar to the one at the beginning. Panel *B* corresponds to an observation from the stable interval: the presence of a soft component is evident, as well as a steepening of the power law. Panel *C*, an observation from the soft branch, shows a spectrum dominated by the soft component, and finally panel *D*, from the low horizontal track, shows again a power law, slightly steeper than panel *A*.

We can identify the horizontal tracks and the stable section as VHS, and the vertical track as HS, identification confirmed by the timing analysis [24]. The LS is not observed here at the beginning, as most of the rising part of the outburst was not observed, while it was observed at the end, after the observations shown here [22].

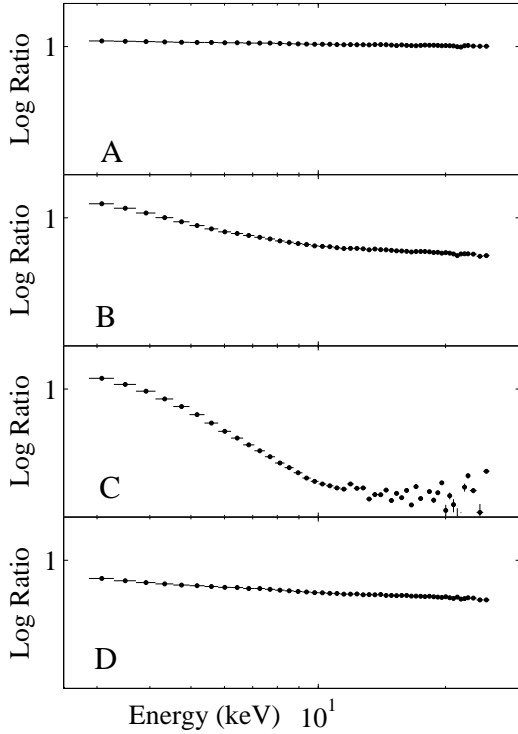


Figure 7. Ratio of the energy spectrum of four representative observations to that of the first observation of the campaign of XTE J1650-500. Panel A: observation on the upper horizontal track in Fig. 6; panel B: observation on the stable interval (see text); panel C: observation from the soft track; panel D: observation from the lower horizontal track.

4.2. GX 339-4

GX 339-4 is historically an important system, as it was the only persistent BHC that showed all spectral/timing states [28,29,27,30,31]. In May 1999, it entered a period of quiescence that lasted until 2002 [32,33]. In March 2002, a new long outburst began and the source was observed regularly by RXTE for more than a year [15,26,25].

Figure 8 shows the PCA light and hardness curves for GX 339-4, where hardness is now the ratio of the counts in the 4.5-8.6 keV band to those in the 2.0-4.6 keV band (from [25]). Large

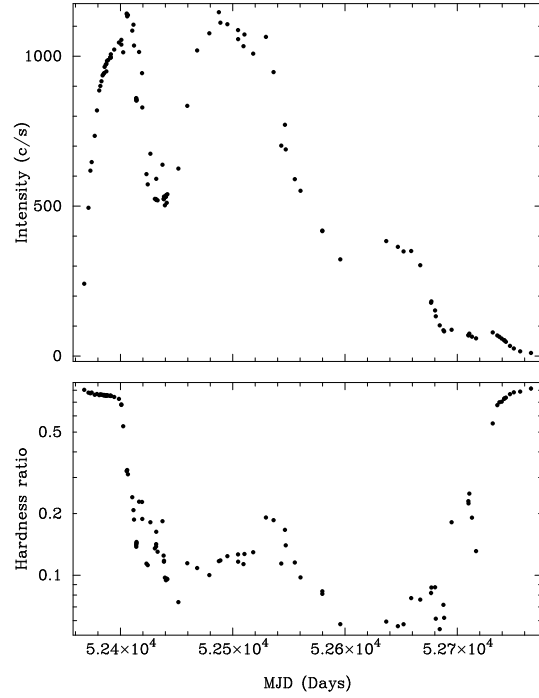


Figure 8. Top panel: PCA slight curve (PCU2 only) for the GX 339-4 RXTE campaign. Each point correspond to one observation. Bottom panel: corresponding hardness curve (see text). (from [25]).

hardness variations are visible. Once again, the spectral changes can be seen better in a HID (Fig. 9). Here the coverage of the outburst started earlier, and the source is observed to start from the bottom right and move upwards along a vertical track, consistent with a constant spectrum and flux variations. After this initial phase, in its general trend the HID is similar to that of XTE J1650-500. First a horizontal track at high count rates shows the source softening. Then there are a few observations spent in a region of lower count rate, followed by a movement onto the soft vertical branch. At the end of the outburst, a low-rate horizontal track is followed to the right, to go back to the initial hardness.

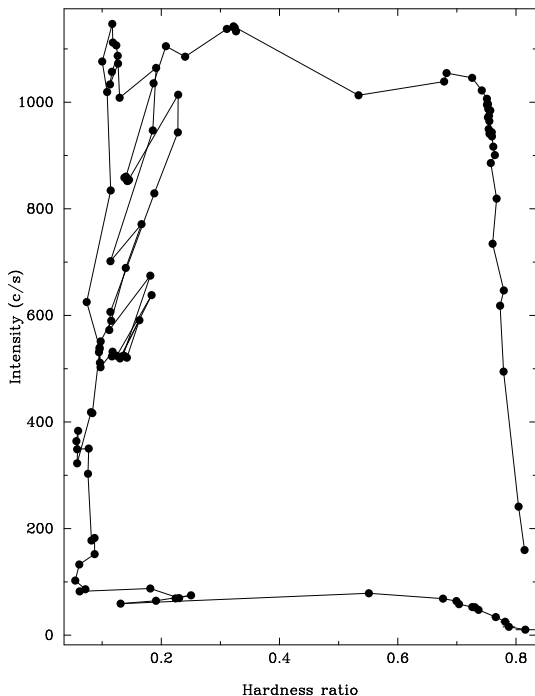


Figure 9. Hardness-Intensity diagram for GX 339-4 (PCU2 only) corresponding to the points shown in Fig. 8 (from [25]).

5. Another look at the canonical states

From the outburst behavior of the two sources examined above, with the excellent coverage provided by RXTE, we can take a fresh look at the canonical states from the spectral point of view. In the following, I present a short summary of work that will be presented in [35]. A schematic HID is shown in Fig. 10. The three states are clearly identified in the diagram:

- *LS*: it is clearly associated only to the beginning and the end phases of the outburst, i.e. to lower accretion rate values, and never observed mixed with the other states. The LS is represented by the black track on the right side of the diagram. This track extends down to very low count rates, spanning three orders of magnitude in the case

of GX 339-4 [25].

- *HS*: associated to the central section of the outburst, it is represented by the gray track on the extreme left, where the soft thermal component completely dominates the spectrum.
- *VHS/IS*: here defined as the central region of the HID, in between the thin LS and HS vertical tracks. There is clearly more than one different instance of VHS/IS, which is reflected by the fact that the definition of VHS/IS which can be found in the literature is sometimes rather vague.

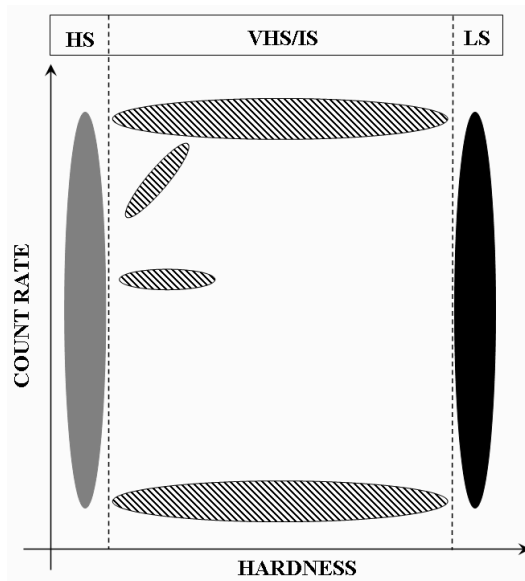


Figure 10. Schematic Hardness-Intensity diagram for a generic BHC.

Although I tried to limit myself to spectral information, it is not possible to leave variability information aside, as it is fundamental in assessing source states. In Fig. 11 I show four representative Power Density Spectra (PDS) from observations of GX 339-4. They correspond to four

observations from the four tracks shown in Fig. 9. The top two PDS, from the right and left vertical tracks, are typical of LS and HS and can be compared to those from [31]. The bottom two, from the top and bottom horizontal tracks, are typical of VHS and IS, as also observed in the past from the same source [27,30].

With this characterization, the VHS/IS, for which Intermediate State is clearly a better denomination, is configured as a transitional state, most notably between LS and HS (or viceversa), but also as a “transient” state which can appear for short times in the middle of an outburst. Whether these three instances of what we call IS are the same physical state is not clear, but needs to be investigated through theoretical models.

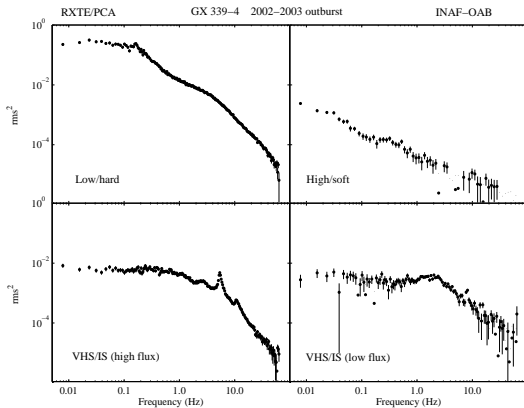


Figure 11. Four characteristic power density spectra for GX 339-4 as observed by RXTE [25]. The upper two panels show examples from the HID hard (LS: left) and soft branch (HS: right). The bottom panels refer to two observations in the VHS/IS, on the high-flux (left) and low-flux (right) branch.

6. Conclusions

In the first part of the paper, I presented recent results on the broad-band spectral distribu-

tion of BHC, made possible by the exceptional combination of instruments on board RossiXTE and especially BeppoSAX. We are now in the condition to test complex physical models to the data, although the limitations of the instruments must be kept into account. The different nature (thermal/non-thermal) of the hard component was examined. In particular, I showed how timing and spectral information available are not consistent in associating the hard component observed in the IS to either that characteristic of the LS or to that of the HS.

The second part was dedicated to presenting basic spectral results from recent RXTE observational campaigns of XTE J1650-500 and GX 339-4. I presented in particular Hardness-Intensity diagrams for the two systems and compared them. From these results, supported by extensive timing analysis only briefly shown here, I present a new phenomenological view of spectral/timing states of BHC, clarifying some of the existing confusion between different flavors of VHS/IS and identifying a partial dependence of state transitions on variations in the mass accretion rate.

7. Acknowledgements

I thank Jeroen Homan, Sabrina Rossi and Elisa Nespoli, who provided the results of their analysis of GX 339-4 and XTE J1650-500.

REFERENCES

1. R.I. Hynes, et al., 2000, *ApJ*, 539, L37
2. J.E. McClintock, et al., 2001, *ApJ*, 555, 477
3. S. Markoff, H. Falcke, R.P. Fender, 2001, *A&A*, 372, L25
4. F. Frontera, et al., 2001a, *ApJ*, 561, 1006
5. F. Frontera, et al., 2003, *ApJ*, 592, 1110
6. A.A. Esin, et al., 2001, *ApJ*, 555, 483
7. F. Frontera, et al., 2001b, *ApJ*, 546, 1027
8. J.B. Dove, et al., 1998, *MNRAS*, 298, 729
9. J.E. Grove, et al., 1998, *ApJ*, 500, 899
10. J. Homan, et al., 2001, *ApJS*, 132, 377
11. T. Belloni, et al., 2000, *A&A*, 355, 271
12. T. Belloni, 1998, in “19th Texas Symposium on Relativistic Astrophysics and Cos-

- mology”, Eds.: J. Paul, T. Montmerle, and E. Aubourg.
13. P. Reig, T. Belloni, M. van der Klis, 2003, A&A, submitted
 14. A. Zdziarski, et al., 2001, ApJ, 554, L45
 15. T. Belloni, et al., 2003, in “New views on Microquasars”, p84.
 16. J. Rodriguez, et al., 2003, A&A, submitted
 17. C. Markwardt, et al., 2001, IAUCirc. 7707
 18. M. Revnivtsev & R. sunyaev, 2001, IAUCirc. 7715
 19. R. Wijnands, et al., 2001, IAUCirc. 7715
 20. J. Homan, et al., 2003, ApJ, 586, 1262
 21. J.M. Miller, et al., 2002, ApJ, 570. L69
 22. E. Kalemci, et al., 2003, ApJ, 586, 419
 23. S. Rossi, et al., 2003, this volume
 24. S. Rossi, et al., 2003, in preparation
 25. E. Nespoli, et al., 2003, in preparation
 26. E. Nespoli, et al., 2003, A&A, submitted
 27. T. Belloni, et al., 1997, A&A, 322, 875
 28. S. Miyamoto, et al., 1991, ApJ, 435, 398
 29. K. Ebisawa, et al., 1994, PASJ, 46, 375
 30. M. Méndez & M. van der Klis, 1997, ApJ, 479, 926
 31. T. Belloni, et al., 1999, ApJ, 519, L159
 32. A.K.H. Kong, et al., 2000, MNRAS, 312, L49
 33. S. Corbel, et al., 2003, A&A, 400, 1007
 34. M. Gilfanov, et al., 1995, NATO ASI Series 450, p331
 35. J. Homan, T. Belloni, 2003, in preparation
 36. Y. Tanaka & W. Lewin, 1995, in “X-ray binaries”, p126
 37. M. van der Klis, 1995, in “X-ray binaries”, p252